The Impact of Patchy Snow Cover on Snow Water Equivalent Estimates Derived from Passive Microwave Brightness Temperatures Over a Prairie Environment

KIM R. TURCHENEK[1], JOSEPH M. PIWOWAR[1], AND CHRIS DERKSEN[2]

ABSTRACT

Considerable seasonal and inter-annual variation in the physical properties and extent of snow cover pose problems for obtaining reliable estimates of quantities and characteristics of snow cover both from conventional and satellite measurements (Goodison and Walker, 1994; Goita et al., 2003). In spite of these challenges, the Climate Research Branch of the Meteorological Service of Canada (MSC) has developed a suite of algorithms to derive snow water equivalent (SWE) estimates from remotely sensed passive microwave imagery (Goodison and Walker, 1994; Derksen et al., 2002; Goita et al., 2003). These algorithms work particularly well over open prairie environments under the assumption of large areas of consistent snow cover (Derksen et al., 2002). While studies have documented underestimation in passive microwave estimates of snow extent in marginal areas when compared to optical satellite data (Derksen et al., 2003b), the accuracy in SWE retrievals under variable and patchy snow conditions is not well understood.

In an effort to better understand how a variable and patchy snow cover impacts remotely sensed SWE retrievals, a field-based experiment was conducted over a patchy snow covered area in February 2005. A systematic sampling strategy was developed over a 1600 km² area in southern Saskatchewan near a calibration/validation flight line used for algorithm development in the 1980s (Goodison and Walker, 1994). Land cover at the sampling sites included fallow and stubble fields, pastures, and shelter belts. A large number of sampling sites contained snow pack layers that included one or more ice lenses.

We verify that the continuous snow cover assumption embedded in the MSC passive microwave SWE algorithm does not produce acceptable results over a patchy snow cover. Several in-situ observations that appear to play an important role in affecting the satellite passive microwave data over a variable snow cover include the presence or absence of an ice lens, the fractional snow covered area, snow depth, and the ground temperature.

Keywords: snow cover, snow water equivalent, passive microwave, remote sensing

INTRODUCTION

Microwave radiation is naturally emitted everywhere on the Earth. Its measurable intensity varies from place to place based on soil types, land covers, snow pack characteristics, and other variables (Goita et al., 1997; Sokol et al., 1999). At microwave frequencies above 15 GHz, the emitted radiation is scattered by snow particles as it passes through the snow pack (Goita et al.,

---

[1] Department of Geography, University of Regina, Regina, Saskatchewan, S4S 0A2
[2] Climate Research Branch, Meteorological Service of Canada, Downsview, Ontario M3H 5T4

1997). Increasing the snow pack depth or grain size results in an increase in scattering and subsequent lower microwave brightness temperatures when measured above the surface (Goita et al., 1997). Wet and/or dense snow packs however, decrease the amount of scattering, and produce near blackbody emissions (Sokol et al., 1999). Complex snow packs, containing numerous layers at different densities, selectively influence microwave radiation, producing inconsistent measurements.

Radiation recorded by a microwave sensor is expressed as a brightness temperature (T_B) in Kelvin units. One parameter commonly derived from remotely sensed brightness temperatures is snow water equivalent (SWE), which is the amount of water stored in a snow pack that is available upon melt.

Intensive research with passive microwave T_B data has focused on empirically derived algorithms used to estimate SWE for validation of ground-truth observations (Goodison and Walker, 1994; Goita et al., 1997; Derksen et al., 2002; 2003a). Currently, the Meteorological Service of Canada (MSC) employs a suite of linear algorithms to retrieve SWE estimates from passive microwave sensors. The MSC algorithms vary according to land cover, with different coefficients used for open prairie, deciduous forest, coniferous forest, and sparse forest (Goita et al., 1997; Singh and Gan, 2000; Derksen et al, 2003a; 2003b). For example, the algorithm used to derive SWE over the open prairie is a vertically polarized T_B gradient ratio (Goodison and Walker, 1994) defined as:

$$SWE \text{ (mm)} = -20.7 - (37v - 19v) * 2.59 \qquad [1]$$

Variables 37v and 19v are the brightness temperatures acquired from vertically polarized frequencies of 37 and 19 GHz, while the coefficients 2.59 and –20.7 are the slope and intercept of the best-fit regression line found between ground and airborne brightness temperatures (Goodison, 1989). Numerous studies have found SWE estimates derived from this algorithm to be within +/– 10–20 mm of in-situ observations (Goodison and Walker, 1994; Derksen et al., 2002; 2003b), however, the MSC algorithm assumes a complete snow cover and the effects of patchy snow cover on SWE estimates are not well understood.

To help understand the relationship between patchy snow covers and remotely sensed SWE estimates, a field campaign to measure SWE in a highly variable snow pack was conducted from February 21st to 23rd, 2005 in southern Saskatchewan. The objectives of this study were to:

i) Compare remotely sensed SWE estimates against ground-truth measurements;
ii) Determine how well the MSC prairie SWE algorithm performs over a patchy snow cover; and
iii) Identify in-situ variables that significantly influence passive microwave SWE estimates over a patchy snow cover.

STUDY AREA

The study area is located approximately 100 km south of Regina, Saskatchewan around the town of Radville and the villages of Pangman and Ceylon (Figure 1). This area was selected because previous research had been performed in this area by Environment Canada. In addition, the snow cover typical of this area has been found to have regions of both patchy and complete snow-cover (Goodison and Walker, 1994; Turchenek, 2004).

The Missouri Coteau, a remnant glacial moraine, cuts across the southwest portion of the study area, forming a low, rolling topography. Although the natural vegetation in this area consists of short grasses, a large portion of the land is under agricultural production, where wheat and other grains are farmed. Pockets of trees and shrubs create shelter belts in areas with higher moisture supply.

8

Relatively short warm summers and long cold winters are characteristic of Saskatchewan's prairies (Hare and Thomas, 1979). With few perennial streams, much of the region's water supply comes in the form of precipitation. However, the annual precipitation in the region is relatively low, and evapotranspiration usually exceeds the annual precipitation, creating an average water deficit by middle to late summer (Laycock, 1972). Most annual precipitation falls in the summer, while February is usually the driest month (Hare and Thomas, 1979).
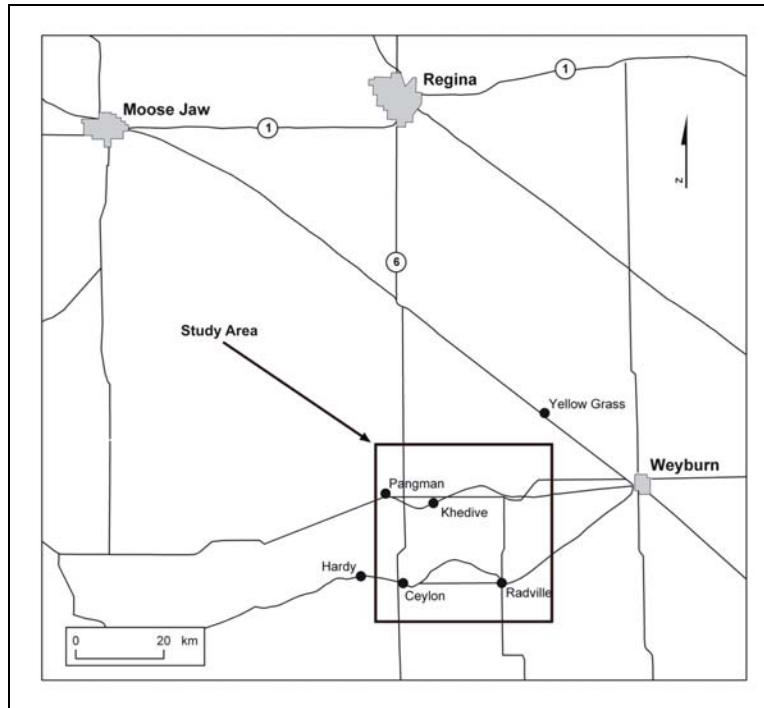

Figure 1: Study area

The winter season provides relatively low amounts of snow. Extended periods of cold, clear weather are interrupted by occasional blizzards with gusting winds. Warming periods are frequent in the early and late winter (Laycock, 1972; Hare and Thomas, 1979; Walker et al., 1995). Wind re-distributes the snow cover by removing snow from one area and depositing it in another. Similarly, warming periods also impact the snow cover through freeze–thaw processes (Laycock, 1972; Walker et al., 1995). As the air and ground temperatures rise, the snow pack melts. When the snow pack re-freezes, it becomes denser and shallower. Thus, along with topographic effects and changes in vegetation, weather systems can impart a considerable variability in snow pack depths and densities.

REMOTE SENSING DATA

Four sets of coincident remote sensing data were analyzed (Table 1). Three data sets were derived from the brightness temperatures collected from the Advanced Microwave Scanning Radiometer for NASA's Earth Observing System (AMSR-E). The first AMSR-E data set includes T_B re-sampled to the 12.5 km Equal Area Scalable Earth Grid (EASE-Grid) (Armstrong and Brodzik, 1995). The second includes AMSR-E T_B re-sampled to the 25 km EASE-Grid and the third AMSR-E data set includes non-gridded T_B swath data. For comparison, a fourth data set of SWE estimates derived from Special Sensor Microwave/Imager (SSM/I) brightness temperatures re-sampled to the 25 km EASE-Grid was included. Although data were acquired for each day of the field campaign, the only remote sensing data analyzed here were those collected on the first

day of the campaign (Feb 21st, 2005). Future research will incorporate the coincident remote sensing data from each date of the field campaign.

Table 1: Remote sensing data used within this study

Data Set Label	Spatial Resolution	Description
1) 12.5k_AMSR-E $_{SWE}$	12.5 km	SWE estimates derived from AMSR-E T_B re-sampled to 12.5 km EASE-Grid
12.5k_AMSR-E $_{18.7v}$	12.5 km	18.7v T_B obtained from AMSR-E re-sampled to 12.5 km EASE-Grid
12.5k_AMSR-E $_{36.5v}$	12.5 km	36.5v T_B obtained from AMSR-E re-sampled to 12.5 km EASE-Grid
2) 25k_AMSR-E $_{SWE}$	25 km	SWE estimates derived from AMSR-E T_B re-sampled to 25 km EASE-Grid
25k_AMSR-E $_{18.7v}$	25 km	18.7v T_B obtained from AMSR-E re-sampled to 25 km EASE-Grid
25k_AMSR-E $_{36.5v}$	25 km	36.5v T_B obtained from AMSR-E re-sampled to 25 km EASE-Grid
3) Swath_AMSR-E $_{SWE}$	24 km x 12 km	SWE estimates derived from AMSR-E T_B that have not been re-sampled
Swath_AMSR-E $_{18.7v}$	24 km	18.7v T_B obtained from AMSR-E that have not been re-sampled
Swath_AMSR-E $_{36.5v}$	12 km	36.5v T_B obtained from AMSR-E that have not been re-sampled
4) 25k_SSM/I $_{SWE}$	25 km	SWE estimates derived from SSM/I T_B re-sampled to 25 km EASE-Grid

METHODS

The analysis procedure was divided into four steps: i) collection of the ground-truth observations, ii) processing of the data sets, iii) comparison with the remotely sensed SWE estimates, and iv) statistical tests. These are discussed in the following subsections.

In-situ Data Collection

The study area was systematically divided into 25 km square grid cells, with the centre of each cell located at 5 km intervals. Field measurements were made nearest the centre of each grid cell as possible. The field campaign was concentrated into a three-day period to minimize changes in snow pack conditions due to melt or fresh snowfall.

Two teams, of 3–4 surveyors each, collected a total of 88 ground observations from 84 sampling sites that covered an area of 1600 km^2. As a control, four of the sites were sampled on consecutive days to ensure data consistency. Included in the 84 sampling sites were 20 sites coincident with an established MSC validation/calibration snow course data archive (Flight Line 603). Comparisons among these data will be the subject of a future communication. The land coverage of the sampling sites included pastures and shelter belts, as well as fallow and stubble fields. The ground-truth data collected from each sampling site included: geographic locations, snow pack profiles, depth measurements, core samples, air and ground temperatures, site photographs, sampling dates and times, and land cover and weather observations. Sampling site locations were recorded using global positioning system (GPS) handsets. Since data for differential corrections were not available, the positions have an approximate accuracy of 10 metres.

Approximately 90% of the sampling sites were found to have patchy snow coverage. As such, one of the first observations made at each site was a visual assessment of the percentage of snow cover. Each team member made this assessment independently and these values were then averaged to reduce bias in this variable. For sites with complete snow cover, a total of 4 snow core samples were collected. This number was reduced proportionally for partially covered sites. For example, only 2 cores were collected from sites determined as having 50% snow coverage, and just 1 core was collected from sites with 25% snow cover. This rationale was used to satisfy the requirement that the cores be taken randomly within each site. Thus, if a site was found to have 50% snow cover, then the probability of randomly selecting a sampling location containing snow is only 50%. In this situation, the 2 core samples that were not actually collected were simply given zero values for their core lengths, depths, weights, and densities.

The core samples were obtained using Eastern Snow Conference (ESC-30) snow core tubes. Measurements from the core samples include the actual depths of the snow packs from where the cores were removed, the lengths of the cores, and their weights. The lengths and weights of the cores were used to calculate the core densities and ground SWE measurements. Snow densities, represented as g/cm^3, were based on the average of the 0 to 4 core samples.

A snow pit was dug at each sampling site and a detailed snow pack profile was made that included the snow pack's total depth, the number of layers and ice lenses within the snow pack, the depth and snow grain size of each layer (using Sears snow crystal screens, labeled with 1–3 mm grids), a qualitative description of each layer, and the air and snow/ground interface temperatures. A total of 16 depth measurements were made around each snow pit using 15-metre long ropes as guides for the purpose of consistently collecting the depth measurements from 30-metre diameter circles. Depth measurements to the nearest one-half centimetre were made using 1-metre-long depth probes. The depth measurements from each site were used to calculate the average depths within the sites, which were then used as representative values for the sampling sites. The average depths are based on the 16 random depth measurements recorded from the circle around the snow pit along with the 0 to 4 depth measurements recorded from the snow core samples.

Other data recorded included the sampling dates and times, weather observations, and land cover types.

In-situ Data Processing

Two data sets were created from the ground sampled data in order to better understand how snow properties over a partial snow cover are manifested in the remotely sensed SWE estimates. In the "Snow-Only" data set, only those snow depth measurements that were greater than zero were included in the average depth, density, and ground SWE calculations. For example, if a site was found to have snow depth readings of 3, 4, 0, 1, and 4 cm, then the average depth for that site was recorded as 3.0 cm ((3 + 4 + 1 + 4) / 4), excluding the zero value. Conversely, the same site in the "Actual-Conditions" data set would have a mean depth of 2.4 cm ((3 + 4 + 0 + 1 + 4 / 5)).

From each of these data sets, four SWE estimates were calculated. The first ground SWE value, "Core_SWE," represents the SWE calculated by using the mean SWE from the snow cores only. The second SWE value, "Derived_SWE," is representative of the mean value for the Core_SWE plus the SWE derived from the 16 depth measurements using the average density for each sampling site. The remaining SWE values, "Fractional_Core_SWE" and "Fractional_Derived_SWE" are represented by the previous SWE values weighted by the Snow_Cover_Percent, respectively. Four SWE values were deemed necessary to investigate the most accurate way of representing SWE over a patchy snow cover.

Remote Sensing Data

The remote sensing images were re-projected to a UTM projection for analysis in ArcGIS. Each pixel centroid was assumed to be a point, and pixel footprints were created using Thiessen polygons. The Thiessen polygon algorithm segments the measurement space into polygons such that every polygon encloses the region closest to each pixel centroid (O'Sullivan and Unwin, 2003). Although the algorithm does not produce perfectly squared pixels, the fact that the algorithm measures the mid-points between the pixel centroids ensures that the spatial resolutions of the remote sensing data sets are preserved.

Following previous research by Goodison and Walker (1995) and Derksen et al. (2002, 2003b), remotely sensed SWE estimates were compared to ground SWE measurements. The remotely sensed estimates found to be within +/–20 mm (the previously determined accuracy of the MSC SWE algorithm) of ground measurements were considered as equivalent. SWE estimates found not to be within the +/–20 mm threshold were considered as anomalous.

Statistical Comparison Tests

Z-tests were performed between the results of the Snow-Only and Actual-Conditions data sets to determine if there were significant differences in algorithm performance between the two ground-truth representations. Linear regression models were developed between the remote sensing data (as the dependant variables) and the ground observations from the coincident sampling sites (as the independent variables).

The linear regression outputs were interpreted following the systematic procedure proposed by Gupta (2000) (Figure 2). The significance of the model fit is analyzed. The model significance explains the deviations of the dependent variables (eg. the SWE estimates and T_B). We used a model significance of 0.10 (90% confidence level) as the cutoff for model acceptance. Models with levels below the 90% confidence level were removed from further analysis.

The next step in interpreting the regression output is to analyze the Adjusted R^2 value from the model summary. This value is sensitive to the addition of irrelevant variables, and is a measure of the proportion of the variance in the dependent variables that are explained by the variations of the independent variables. For example, an Adjusted R^2 value of 0.500 suggests that 50% of the variance in a SWE estimate is explained by the variation in the ground-truth measurements.

The third interpretation step involves identifying the reliability of the individual coefficients for the independent variables. The Beta values included in the coefficients output indicate the predicted coefficients for the model along with their standard errors and significances. Similar to the significance of the model fit, if a coefficient results in a significance value above 0.10, then it can be concluded that the independent variable is not significant at a 90% level of confidence.

Table 2 provides an instructive example of how an output coefficient table is analyzed. The SWE predicted by the model is specified by the Constant's Beta coefficient, 30.5 mm. The standard error of this prediction is 1.9 mm of SWE. The next step is to identify the significance of the independent variables' Beta coefficients. In this example, a coefficient of .149 for the average snow pack depth is found to be significant at a 95% level of confidence (sig. = .043), but the coefficient of –2.899 for the average density is irrelevant (sig. = .776) towards the predicted SWE value.

Table 2: Example coefficient table output

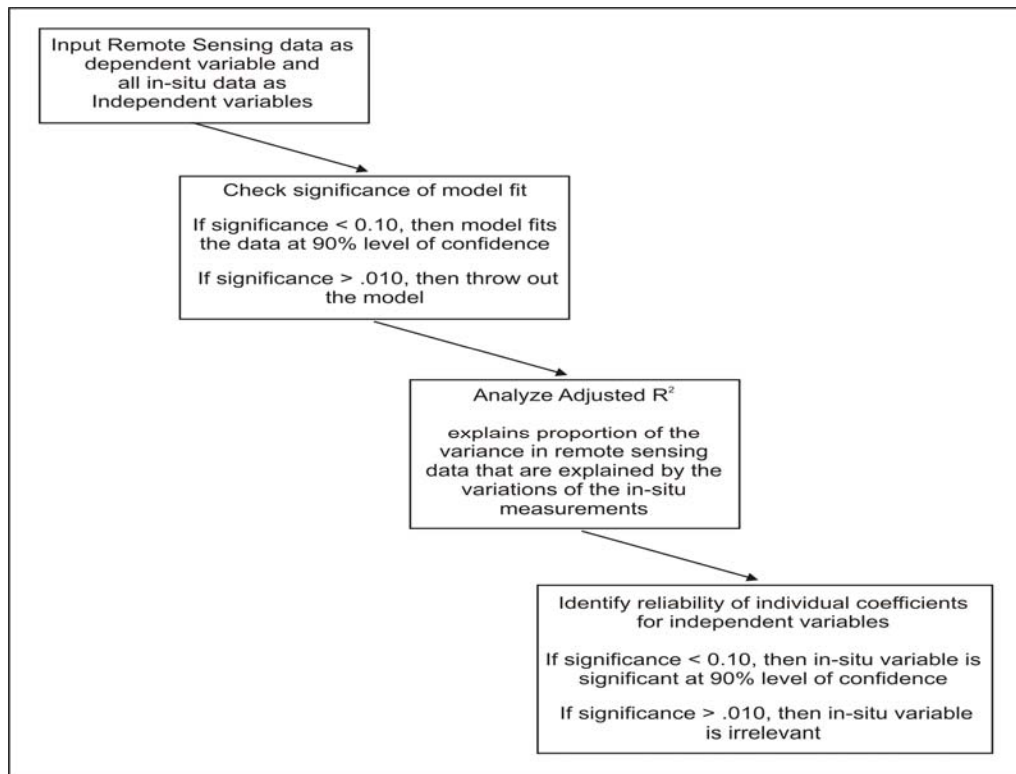| Model	Unstandardized Coefficients		Significance
	Beta	St. Error	
Constant (predicted SWE value)	30.5	1.9	—
Depth	.149	.111	.043
Density	–2.899	10.148	.776

12

Figure 2: Flow chart of regression analyses

RESULTS

The results are presented in two parts. First, the remotely sensed SWE estimates are compared with the SWE measurements obtained from the coincident sampling sites. This is followed by an analysis of the linear regression models.

In-situ *vs.* Remotely Sensed SWE Estimates

The SSM/I and swath AMSR-E SWE data provided the closest estimates to both in-situ data sets. This was expected, because: i) the MSC algorithm used to derive SWE estimates was actually developed for SSM/I T_B, and ii) the swath AMSR-E T_B have not been re-sampled, thus, they are truer representations of the interaction between the sensor and the ground surface. Tables 3 and 4 illustrate the number (and percentage in brackets) of sampling sites that were found to be equivalent (i.e. within +/–20 mm SWE) to the remotely sensed SWE estimates. Table 3 shows the results of the Snow-Only data set, while Table 4 presents the results of the Actual-Conditions data set. These results also show a slight increase in algorithm agreement when only the amount of snow found at each sampling site is included in the ground-truth observations (i.e. Core_SWE from Table 3 vs. Table 4).

Table 3: Number of equivalent Snow-Only coincident sites (n=88)

SWE Calculation	SSM/I	12.5k AMSR-E	25k AMSR-E	Swath AMSR-E
Core_SWE	55 (63%)	42 (48%)	20 (23%)	56 (64%)
Fractional_Core_SWE	50 (57%)	29 (33%)	11 (13%)	49 (56%)
Derived_SWE	58 (66%)	32 (36%)	15 (17%)	54 (61%)
Fractional_Derived_SWE	45 (51%)	24 (27%)	7 (8%)	45 (51%)

Table 4: Number of equivalent Actual-Conditions coincident sites (n=88)

SWE Calculation	SSM/I	12.5k AMSR-E	25k AMSR-E	Swath AMSR-E
Core_SWE	51 (58%)	34 (39%)	13 (15%)	52 (59%)
Fractional_Core_SWE	44 (50%)	27 (31%)	10 (11%)	45 (51%)
Derived_SWE	45 (51%)	26 (30%)	9 (10%)	49 (56%)
Fractional_Derived_SWE	33 (38%)	23 (26%)	7 (8%)	40 (45%)

By weighting the in-situ SWE values by the percentage of snow cover found at the sites (i.e. reading down each column) the agreement with the remote sensing estimates decreases by an average of approximately 10% in the Snow-Only data set, and by an average of approximately 7% in the Actual-Conditions data set. Further, the remote sensing SWE algorithm generally had a higher level of agreement with Core_SWE measurements than with Derived_SWE values.

Therefore, for a patchy snow cover, it appears that the MSC SWE algorithm had the closest agreement with ground SWE measurements based only on the core samples

Further analyses using only these Core_SWE measurements found that, on average, the remote sensing algorithm tended to overestimate the patchy in-situ SWE measurements in all cases (Table 5). This was not surprising since the remote sensing algorithm was originally derived for a complete snow cover.

Table 5: Mean differences in SWE values between remote sensing estimates and in-situ measurements (for core samples only)

	SSM/I	12.5k AMSR-E	25k AMSR-E	Swath AMSR-E
Snow-Only $_{Core\_SWE}$	4.8	17.7	32.1	5.4
Actual-Conditions $_{Core\_SWE}$	8.7	21.6	35.9	9.3

We also wanted to examine the effect that varying land covers had on the spaceborne SWE estimates. The ranges in ground SWE measurements were very high, particularly when the sampling sites included shelter belts and fallow fields, which were found to have drastically different snow conditions than stubble fields and pastures. Table 6 shows that there is little difference in the mean SWE values representative of stubble fields (26.1 mm) and pastures (23.0 mm), but great disparity between these values and fallow fields (1.7 mm) and shelter belts (94.8 mm).

14

Table 6: Actual-Conditions SWE, depth, and density measurements by land cover type

Land Cover	n	SWE (mm)	Depth (cm)	Density (g/cm^3)
Stubble	54	mean = 26.1	mean = 7.9	mean = 0.226
		min = 1.3	min = 1.0	min = 0.026
		max = 66.3	max = 19.0	max = 0.511
Fallow	15	mean = 1.7	mean = 0.8	mean = 0.054
		min = 0	min = 0	min = 0
		max = 8.8	max = 4.7	max = 0.265
Pasture	12	mean = 23.0	mean = 6.7	mean = 0.219
		min = 5.1	min = 1.8	min = 0.110
		max = 44.1	max = 16.4	max = 0.364
Shelter Belt	2	mean = 94.8	mean = 26.8	mean = 0.292
		min = 75.6	min = 22.7	min = 0.267
		max = 114.0	max = 30.9	max = 0.316

Linear Regression Models

   Linear regressions were performed using the Statistical Package for the Social Sciences (SPSS) software. The regressions were performed using the remotely sensed SWE estimates and brightness temperatures as the dependent variables and the in-situ observations as the independent variables. Analyses were again performed between the Snow-Only and Actual-Conditions data sets. Table 7 lists and describes the in-situ observations used in all of the regression models.

Table 7: Measured snow properties used in linear regression models

Independent variable	Variable Type	Description
Percent_Snow_Cover	Ratio	Percentage of snow cover found at each sampling site.
Depth	Ordinal	Mean snow pack depth of each site.
Density	Ratio	Mean snow pack density of each site.
Air_Temp	Interval	Air temperature recorded at each site.
Ground_Temp	Interval	Snow/ground interface temperature recorded from the snow pit.
Num_Layers	Ordinal	Number of snow pack layers found in the snow pit.
Land_Cover	Nominal	Type of land cover.
Ice_Lens	Binary/Nominal	Indicates whether or not one or more ice lenses were found in the snow pack of the snow pit.
Num_Lenses	Ordinal	Number of ice lenses found in the snow pack of the snow pit.
Total_Lens_Thickness	Ordinal	Total ice lens thickness found within the snow pack of the snow pit.

   The linear regression analyses found that snow pack densities from the Actual-Conditions data set were significantly positively correlated with SWE estimates derived from the Swath AMSR-E data. This was expected since dense and complex snow packs have been shown to amplify scattering and tend to produce remotely sensed SWE overestimates (Sokol et al., 1999). The Swath AMSR-E imagery was the only remote sensing data set to show such a statistically significant correlation, likely because — since they had not been re-sampled to the EASE-Grid — these data were closer representations of the original Earth radiances originally detected by the sensor.

Table 8 shows the regression results between the Swath AMSR-E SWE estimates and both the Snow-Only and Actual-Conditions data sets. The Model Fit shows that both data sets match the satellite estimates at 99% levels of confidence. From the Unstandardized Beta Coefficients we see that the only significant variables are the percentage of snow cover, and whether or not one or more ice lenses were found in the snow pit. Interestingly, density in the Snow-Only data set appears not to make a significant contribution, while it is found to be significant at a 90% level of confidence in the Actual-Conditions data set. The Model Summaries indicate that the proportion of the variance in the satellite estimates that is explained by the ground observations are just 15.8% and 17.9% for the Snow-Only and Actual-Conditions data sets, respectively.

Table 8: Regression results between Swath AMSR-E SWE estimates and in-situ observations
(significant coefficients are shown in bold italics)

Swath_AMSR-E $_{SWE}$	Snow-Only			Actual-Conditions		
1) Model Fit	.008			.004		
2) Model Summary (Adjusted R^2)	.158			.179		
3) Coefficients	Beta	St. Error	Sig.	Beta	St. Error	Sig.
▪ Constant (Predicted SWE)	32.646	2.280	—	32.552	2.140	—
▪ ***Snow_Cover_Percent***	***8.508***	***4.276***	***.050***	***10.079***	***4.310***	***.022***
▪ Depth	.143	.220	.518	.187	.216	.390
▪ ***Density***	−6.009	6.646	.369	***−19.131***	***11.357***	***.096***
▪ Air_Temp	−.050	.306	.870	−.026	.302	.932
▪ Ground_Temp	−.162	.492	.743	−.257	.489	.601
▪ Num_Layers	.371	1.500	.805	.691	1.498	.646
▪ Land_Cover	−1.555	1.376	.262	−1.490	1.355	.275
▪ ***Ice_Lens***	***−7.354***	***3.369***	***.032***	***−6.738***	***3.267***	***.043***
▪ Num_Lenses	.563	3.205	.861	−.151	3.204	.963
▪ Total_Lens_Thickness	.108	.647	.868	.214	.643	.740

Similar regressions were run between all of the remote sensing and in-situ data sets. The results are summarized in Table 9. Regression models derived for the 12.5k AMSR-E $_{18.7v}$ and 25k AMSR-E $_{SWE}$ data were not statistically significant. Regressions from the AMSR-E T_B found that the 18.7v T_B resulted in having more significant variables than those collected from the 36.5v T_B. While the Snow_Cover_Percent, and Ice_Lens variables were found to be significant in both T_B regressions, Depth and Ground_Temp were found to also be significant in the 18.7v T_B regression. With the 12.5k AMSR-E data it is interesting to note that in comparison to the non-gridded Swath_AMSR-E analyses a completely different set of variables, except for the binary variable Ice_Lens, was found to be significant. The significant variables in this data set include: Depth, Air_Temp, Land_Cover, and Ice_Lens. However, as these data have been re-sampled, there is less confidence in these regression results compared to those of the swath results. Unlike the 12.5k AMSR-E regression results, the 25k AMSR-E $_{18.7v}$ T_B were found to be significant, and the 36.5v T_B were marginally significant. The 25k SSM/I SWE regressions produced nearly identical results between the Snow-Only and Actual-Conditions data sets.

Table 9: Regression results between remotely sensed SWE estimates and in-situ observations (• denotes a statistically significant correlation)

	Swath AMSR-E SWE		Swath AMSR-E 18.7v		Swath AMSR-E 36.5v		12.5k AMSR-E SWE		12.5k AMSR-E 18.7v		12.5k AMSR-E 36.5v		25k AMSR-E SWE		25k AMSR-E 18.7v		25k AMSR-E 36.5v		25k SSM/I SWE	
	S-O	A-C	S-O	A-C	S-O	A-C	S-O	A-C	S-O	A-C	S-O	A-C	S-O	A-C	S-O	A-C	S-O	A-C	S-O	A-C
1) Model Fit	•	•	•	•	•	•	•	•			•	•			•	•	•	•	•	•
2) Model Summary (Adjusted R^2)	0.2	0.2	0.3	0.3	0.2	0.3	0.3	0.3			0.3	0.3			0.3	0.3	0.1	0.1	0.1	0.1
3) Coefficients																				
▪ Snow_Cover_Percent	•	•	•	•	•	•													•	•
▪ Depth			•	•			•	•			•	•					•	•		
▪ Density		•		•		•					•	•								
▪ Air_Temp							•	•												
▪ Ground_Temp			•	•													•	•	•	•
▪ Num_Layers																				
▪ Land_Cover							•	•			•	•								
▪ Ice_Lens	•	•	•	•	•	•	•	•			•	•			•	•	•	•	•	•
▪ Num_Lenses																	•	•		
▪ Total_Lens_Thickness																				

S-O: Snow-Only
A-C: Actual Conditions

CONCLUSIONS AND DISCUSSION

Although statistically significant models were established between many of the remote sensing and in-situ data sets, the proportion of the variance in the satellite estimates that could be explained by the ground observations (i.e. the Model Summaries) was, at most, 0.31. This suggests that either the ground data are insufficient for deriving SWE from spaceborne passive microwave observations or that the remote sensing data were inappropriate. We know from previous research (reviewed earlier) that it is possible to obtain reliable SWE estimates through remote sensing, so we must conclude that there were problems with remote sensing data we used in this experiment. Specifically, the continuous snow cover assumption embedded in the MSC passive microwave SWE algorithm does not produce acceptable results over a patchy snow cover. The poor performance of the MSC SWE algorithm for each remote sensing data set evaluated confirms that the algorithm fails under patchy and variable snow conditions.

In spite of the poorly articulated regression models, there were several in-situ observations that appear to play an important role in affecting the satellite passive microwave data. The presence or absence of an ice lens in the snow pack was consistently identified as a significant coefficient in the regression analyses. Other observations that may prove to be useful include the percent snow cover, snow depth, and the ground temperature. These will need to be investigated further.

Consideration of patchy snow cover is challenging from a ground sampling perspective, however this study shows that the actual conditions found at each sampling site must be incorporated in ground-truth data sets when collecting observations over a partial snow cover. Subsequent analysis will focus on using optical data to determine snow cover fraction within a passive microwave grid cell to greater quantify the impact of patchy snow cover.

ACKNOWLEDGEMENTS

REFERENCES

Armstrong, R. L. and M. J. Brodzik, 1995. An Earth-gridded SSM/I data set for cryospheric studies and global change monitoring, *Advances in Space Research* **16(10)**: 155–163.

Derksen, C., A. Walker, E. LeDrew, B. Goodison, 2002. Time-series analysis of passive-microwave-derived central North American snow water equivalent imagery, *Annals of Glaciology*, **34**: 1–7.

Derksen, C., A. Walker, B. Goodison, 2003a. A comparison of 18 winter seasons of in situ and passive microwave-derived snow water equivalent estimates in Western Canada. *Remote Sensing of Environment*, **88**: 271–282.

Derksen, C., and A. Walker, E. LeDrew, B. Goodison, 2003b. Combining SMMR and SSM/I Data for Time Series Analysis of Central North American Snow Water Equivalent. *Journal of Hydrometeorology*, **4**: 304–316.

Goita, K., A.E. Walker, B.E. Goodison, and A.T.C. Chang, 1997. Estimation of Snow Water Equivalent in the Boreal Forest Using Passive Microwave Data. *Proceedings, GER '97*

(International Symposium: Geomatics in the Era of Radarsat), Ottawa, Canada, May 25–30, 1997. CD-ROM published by Natural Resources Canada and National Defence.

Goita, K., A. Walker, B. Goodison, 2003. Algorithm development for the estimation of snow water equivalent in the boreal forest using passive microwave data. *International Journal of Remote Sensing* **24(5)**: 1097–1102.

Goodison, B., 1989. Determination of areal snow water equivalent on the Canadian Prairies using passive microwave satellite data. Proceedings, *1989 International Geoscience and Remote Sensing Symposium*, Vancouver. **3**:1243–1246.

Goodison, B.E. and A.E. Walker, 1994. Canadian development and use of snow cover information from passive microwave satellite data. In *Passive Microwave Remote Sensing of Land-Atmosphere Interactions*, Choudhury, B.J., Y.H. Kerr, E.G. Njoku, and P. Pampaloni (eds.), VSP, Utrecht, The Netherlands, 245–262.

Gupta, V., 2000. *Regression explained in simple terms*. Obtained online on April 24, 2005, from http://www.telecom.csuhayward.edu/~esuess/Links/Software/RegressionExplained/regression_explained.doc

Hare, F.K. and M.K. Thomas, 1979. *Climate Canada, 2nd Ed.*, Canada: Wiley.

Laycock, Arleigh H., 1972. The Diversity of the Physical Landscape. In *The Prairie Provinces*, Smith, P.J. (ed.), University of Toronto Press.

O'Sullivan, David, and David J. Unwin, 2003. *Geographic Information Analysis*, Hoboken, NJ: Wiley.

Singh, Purushottam Raj and Thian Yew Gan, 2000. Retrieval of Snow Water Equivalent Using Passive Microwave Brightness Temperature Data. *Remote Sensing of Environment*, **74**: 275–286.

Sokol, J., T.J. Pultz, and A.E.Walker, 1999. Passive and Active Spaceborne Microwave Remote Sensing of Snow Cover. *Proceedings, 4th International Spaceborne Remote Sensing Conference/21st Canadian Symposium on Remote Sensing*.

Turchenek, Kim R., 2004. Validation of Snow Water Equivalents Derived from Passive Microwave Brightness Temperatures over a Prairie Environment. Unpublished Undergraduate Thesis, submitted to and accepted by the Department of Geography at the University of Regina, Saskatchewan.

Walker, Anne, Barry Goodison, Michael Davey and David Olson, 1995. *Atlas of Southern Canadian Prairies Winter Snow Cover from Satellite Passive Microwave Data: November 1978 to March 1986*, Downsview, Canada: Atmospheric Environment Service, Environment Canada.